ChemComm

Accepted Manuscript

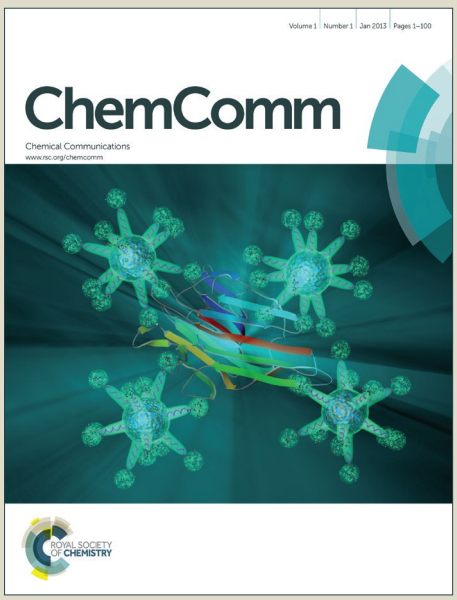

ROYAL SOCIETY OF CHEMISTRY

www.rsc.org/chemcomm

ChemComm

COMMUNICATION

A room temperature approach for the fabrication of aligned TiO_2 nanotube arrays on transparent conducting substrate†

Received 00th January 20xx,
Accepted 00th January 20xx

DOI: 10.1039/x0xx00000x

www.rsc.org/

Ruosha Zeng,[‡ab] Ke Li,[‡bc] Xia Sheng,[b] Liping Chen,[b] Haijiao Zhang[a] and Xinjian Feng[*b]

A novel solution approach is reported to fabricate TiO_2 nanotube arrays on transparent conductive substrates via in-site conversion from nanowires. The as-prepared nanotube arrays not only demonstrate larged surface area in comparison with the primary NWs, but also longer charge carrier lifetime than that of randomly packed nanoparticle films.

In the past two decades nanostructured TiO_2 has been the most widely used electrode material in artificial photosynthesis, solar cells, water splitting and electrical energy storage devices.[1-5] Recently, vertically aligned one dimensional (1D) TiO_2 nanowire (NW) arrays that offer directed charge transport path to the electrode substrate has received substantial attentions.[6-13] Various approaches, such as hydrothermal and solvothermal methods have been reported for the synthesis of TiO_2 NW arrays on transparent conducting substrate.[8-13] Moreover, their unique optical and electrical properties have also been demonstrated. For example, Feng *et. al*. have demonstrated that the electron transport property of single-crystal rutile TiO_2 NW arrays is two orders of magnitude higher than that in the randomly packed nanoparticle (NP) films.[13] Nevertheless, the relatively low surface area caused from the free space between NWs is one of the key issues that limit its broad utility. In order to address this problem, common approaches is to increase the length of NWs, assemble 1D NWs into 3D branched structure, or prepare NWs with mesoporous structure.[14-19]

The fabrication of 1D nanotube (NT) array structure is a good approach to enlarge the surface area. Electrochemical anodic oxidation and template-assisted methods are the most commonly used approaches for NT arrays synthesis.[20-23] These approaches commonly require a high temperature treatment to crystalize the as-anodized amorphous NTs and can only produce NTs in polycrystalline nature. Recently, an in-situ conversion strategy was reported.[24-26] In this process, TiO_2 NTs were fabricated via etching TiO_2 NWs in a strong acidic HCl solution under hydrothermal condition. Herein we demonstrate a simple room-temperature solution approach to fabricate highly crystallized TiO_2 NT arrays from NWs at room-temperature via an anisotropic etching strategy. The obtained TiO_2 NT arrays display regular rectangular cross-section and have much enlarged surface area. Moreover, we demonstrate that the NT arrays have much longer charge carrier lifetime than that of NP films. Our method is simple and the as-prepared NT arrays have the potential to boost the performance of 1D nanostructured electrodes in photovoltaic and photoelectorchemical devices.

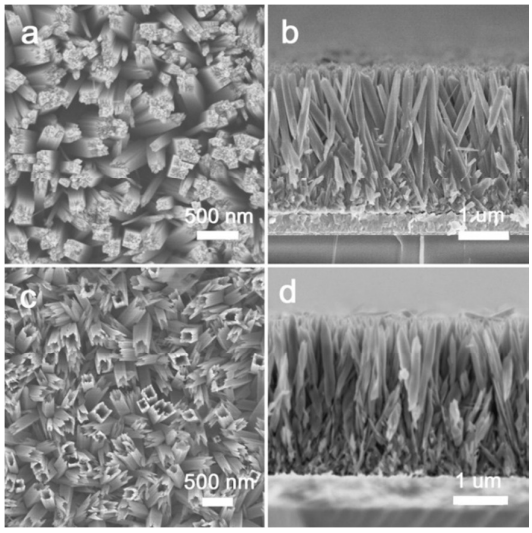

Fig. 1 (a) and (b) are, respectively, SEM top and side views of the as-synthesized TiO_2 NW arrays on FTO substrate; (c) top view and (d) cross-section view of the TiO_2 NT arrays prepared via in-situ conversion from NW arrays shown in (a) and (b).

[a] *College of Environmental and Chemical Engineering, Shanghai University, Shanghai 200444, P. R. China.*
[b] *College of Chemistry, Chemical Engineering and Materials Science, Soochow University, Suzhou 215123, P. R. China. E-mail: xjfeng@suda.edu.cn*
[c] *Nano Science and Technology Institute, University of Science and Technology of China, Suzhou 215123, P. R. China.*
† Electronic Supplementary Information (ESI) available: Experimental procedures and characterization data. See DOI: 10.1039/x0xx00000x
‡ R. Z. and K. L. contributed equally to this work

Rutile TiO_2 NW arrays grown on the F-doped tin oxide (FTO) coated glass substrate were firstly prepared via a conversional hydrothermal method.[8] As can be seen from Fig. 1a and b, the aligned NWs have smooth sidewall but rough top surface. The diameter and length of NWs is about 150-200 nm and 3 µm, respectively. In-situ conversion of NWs into NTs was carried out by simply immersing the as-prepared TiO_2 NW arrays in an aqueous solution of NH_4OH/H_2O_2 at room-temperature (experimental details are included in the Electronic Supplementary Information ESI†). Fig. 1c and d are, respectively, top and side SEM views of the nanostructured film after 90 min treatment, showing that uniform arrays of NTs was prepared. The diameter of the NTs is about 150-200 nm. Compared to the NWs, the diameter, the rectangular shape and the uniform alignment were maintained.

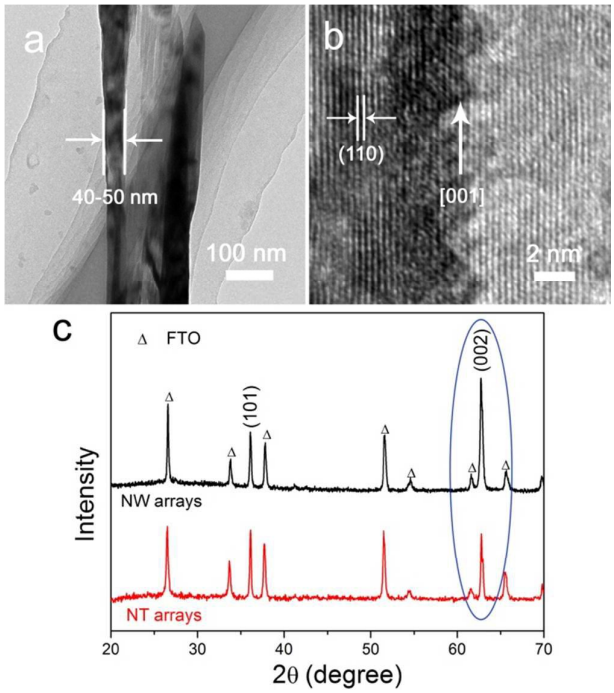

Fig. 2 TEM (a) and high resolution TEM (b) images of the as-prepared rutile TiO_2 NT; (c) XRD patterns of the 1D TiO_2 nanoarray structure before (black line) and after conversion (red line).

The as-prepared NT is further characterized by using transmission electron microscopy (TEM). As shown in Fig. 2a, the wall thickness of NT is within a range of 40-50 nm. The well-crystallized TiO_2 NT has a side surface of {110} crystal facet and a preferred [001] orientation according to high-resolution TEM analysis (Fig. 2b). Fig. 2c compares the X-ray diffraction (XRD) patterns of 1D TiO_2 NW and NT arrays. All of these peaks can be indexed to tetragonal rutile TiO_2 (JCPDS file no. 73-1232), indicating that the crystal phase was preserved after the conversion. It is worth to note that the intensity of the representative (002) peak of 1D TiO_2 nanoarrays become much weaker after the conversion, which confirms that the core of the NWs have been greatly diminished. The surface area of the as-prepared TiO_2 NT arrays were measured by using dye desorption experiment. According to UV-Vis spectra of dye solutions that shown in Fig. S1 (ESI†), the values of 6.4 and 12.4 nmol/cm^2 dye molecule coverage on NW and NT arrays were calculated, respectively, which confirms that the surface area were greatly enlarged after the formation of nanotube arrays.

The formation mechanism of TiO_2 NTs was further studied and found to be closely related to the growth behavior of NWs. Fig. 3a and b show the schematics and the corresponding SEM images of NWs obtained after 1 h and 4 h growth. It can be clearly seen that the NWs have a very small diameter at the initial growth stage (Fig. 3a), and then they grow (aggregate) into one wire via possible oriented attachment mechanism. The diameters of NWs keep increasing with growth time and reach to about 150-200 nm after 4 h (Fig. 3b). On the basis of this growth behavior, numerous defects that caused from crystal lattice mismatch or dislocation during the aggregation of thin NWs will unavoidably exist inside the bulk of NWs, while by contrast, the side walls of NWs has a much higher degree of crystallinity.

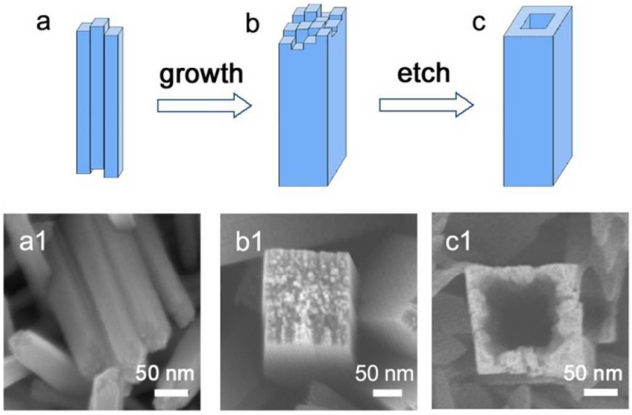

Fig. 3 Schematic illustrations of the morphology evolution of NW. (a) and (a1) are NWs obtained after 1 hour growth, (b) and (b1) are NWs obtained after 4 hours growth; (c) and (c1) are NTs that converted from NW after 90 min treatment.

The subsequent formation of NTs can be ascribed to the selective etching of NWs resulting from the difference in surface energy between side (110) and top (001) top facets as well as these lattice defects inside TiO_2 NWs. In our study, H_2O_2 /NH_4OH mixture is used as the etching solution. Generally, H_2O_2 can dissolve rutile TiO_2 and form a Ti^{4+}- H_2O_2 complex at room temperature via a possible reaction:[27,28] $Ti^{4+} + H_2O_2 + 2H_2O \rightarrow TiO_2 . H_2O_2 + 4H^+$.The presence of NH_4OH inside the solution will promote the forward chemical reaction by neutralizing the H^+. As we know, the surface energy of rutile TiO_2 NWs follows the sequence of (110) < (100) < (001),[29] as a result, the etching rate of the top (001) high energy crystal facet should be much higher than the (110) side surfaces when TiO_2 NWs is treated in H_2O_2/NH_4OH aqueous solution. This result is coincident with XRD analysis, (Fig. 2c) i.e. the intensity

of (002) peak of NWs become much weaker after the formation of NTs. At the same time, the presence of defects inside the bulk of NWs will promote such etching process along the [001] direction because chemical etching commonly takes place preferentially at the defect sites. Thus the solid NWs were converted into regular hollow NTs after treatment (Fig. 3c).

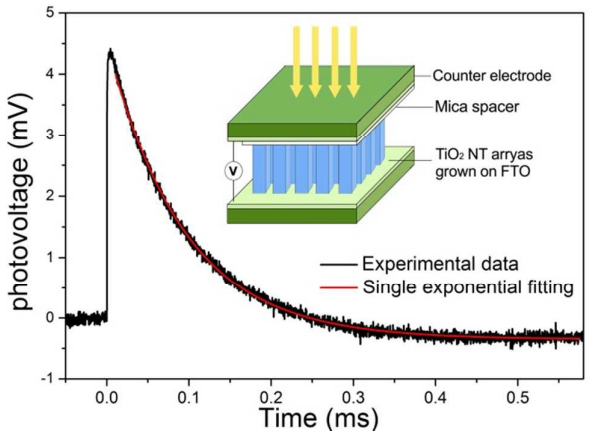

Fig. 4 TPV spectra of the TiO_2 NT arrays and single exponential fitting curve; inset: the diagram of TPV measurement device.

Charge carriers recombination of electrode materials is a major determination of photoelectorchemical devices performance. To understand the charge carrier recombination in TiO_2 NTs, they were analyzed by using transient photovoltage (TPV) spectroscopy. The diagram of TPV measurement is shown in the inset of Fig. 4. The obtained NTs grown on FTO substrate and a bare FTO glass are used as working electrode and counter electrode, respectively. A layer of mica spacer is used to prevent the photo-generated charge-carries in the TiO_2 from directly injecting into the counter electrode. When the sample is illuminated by a pulsed laser, electron and hole pairs will be generated and transport along the nanotubes. Since TiO_2 is an n-type semiconductor with much faster electron diffusion rate than that of holes, the electrons and holes can thus be separated, and the photovoltage is detected. After the charge carrier separation, the electrons and holes undergo a recombination process, which can be recorded and reflected from the TPV decay curve.[30-33] In principle, the photovoltage decay follows the law of single exponential process. The number of recombined electrons (N) can be expressed as:

$$N = N_0 e^{-At}$$

Where N_0 is the number of total photogenerated electrons. A is the Einstein decay coefficient. When $N = N_0/e$, the t is defined as recombination lifetime (τ_r). Fig. 4 is the experimental TPV spectrum of the obtained NTs and the best fitting curve. The τ_r is calculated to be about 0.1 ms. In comparison, a τ_r of 0.06 ms was obtained from randomly packed rutile TiO_2 NP films with the controlled measurement (Fig. S2, ESI†). The longer lifetime of photogenerated charge carrier in TiO_2 NTs can be attributed its 1D directed charge transport path, which facilitates the effective photogenerated charge carrier separation.

In summary, we have reported a simple room-temperature approach for the fabrication of highly crystallized TiO_2 NT arrays on transparent conductive substrates via in-situ conversion of 1D NW arrays. Our experimental results show that the difference in surface energy of crystal facets and the numerous defects inside NWs are crucial for this morphology conversion. The as-prepared NTs show regular rectangular cross-sections with wall thickness of about 40-50 nm and much enlarged surface area. Moreover, its photogenerated charge carriers lifetime is found to be much longer than that of nanoparticle films, which can be attributed to the directed charge transport path. This conversion strategy is simple and is expected to be applied to the formation of other metal oxide nanotubes. The achieved NT arrays will be of broad academic and industrial interest, for example for the application in solar cells, water splitting and energy storage devices.

X. F. acknowledges financial support from the National Natural Science Foundation of China (21371178), the Jiangsu Province Science Foundation for Distinguished Young Scholars (BK20150032), and the Chinese Thousand Youth Talents Program (YZBQF11001). X. S. acknowledges financial support from the National Natural Science Foundation of China (21501193).

References

1 B. O'regan and M. Grätzel, *Nature*, 1991, **353**, 737-740.
2 E. J. Crossland, N. Noel, V. Sivaram, T. Leijtens, J. A. Alexander-Webber and H. J. Snaith, *Nature*, 2013, **495**, 215-219.
3 J. Burschka, N. Pellet, S. J. Moon, R. Humphry-Baker, P. Gao, M. K. Nazeeruddin and M. Grätzel, *Nature*, 2013, **499**, 316-319.
4 A. Fujishima and K. Honda, *Nature*, 1972, **238**, 37-38.
5 M. R. Hoffmann, S. T. Martin, W. Y. Choi and D. W. Bahnemann, *Chem. Rev.*, 1995, **95**, 69-96.
6 H. S. Kim, J. W. Lee, N. Yantara, P. P. Boix, S. A. Kulkarni, S. Mhaisalkar, M. Grätzel and N. G. Park, *Nano Lett.*, 2013, **13**, 2412-2417.
7 Y. J. Hwang, C. Hahn, B. Liu and P. Yang, *ACS Nano*, 2012, **6**, 5060-5069.
8 B. Liu and E. S. Aydil, *J. Am. Chem. Soc.*, 2009, **131**, 3985-3990.
9 X. Feng, K. Shankar, O. K. Varghese, M. Paulose, T. J. Latempa and C. A. Grimes, *Nano Lett.*, 2008, **8**, 3781-3786.
10 J. T. Park, R. Patel, H. Jeon, D. J. Kim, J. S. Shin and J. H. Kim, *J. Mater. Chem.*, 2012, **22**, 6131-6138.
11 M. Yang, B. Ding, S. Lee and J.-K. Lee, *J. Phys. Chem. C*, 2011, **115**, 14534-14541.
12 D. D. Qin, Y. P. Bi, X. J. Feng, W. Wang, G. D. Barber, T. Wang, Y. M. Song, X. Q. Lu and T. E. Mallouk, *Chem. Mater.*, 2015, **27**, 4180-4183.
13 X. Feng, K. Zhu, A. J. Frank, C. A. Grimes and T. E. Mallouk, *Angew. Chem. Int. Ed.*, 2012, **51**, 2727-2730.
14 C. Xu, J. Wu, U. V. Desai and D. Gao, *J. Am. Chem. Soc.*, 2011, **133**, 8122-8125.

15 X. Sheng, D. He, J. Yang, K. Zhu and X. Feng, *Nano Lett.*, 2014, **14**, 1848-1852.
16 I. S. Cho, Z. Chen, A. J. Forman, D. R. Kim, P. M. Rao, T. F. Jaramillo and X. Zheng, *Nano Lett.*, 2011, **11**, 4978-4984.
17 W. Q. Wu, H. S. Rao, Y. F. Xu, Y. F. Wang, C. Y. Su and D. B. Kuang, *Sci. Rep.*, 2013, **3**, 1892.
18 X. Zheng, Q. Kuang, K. Yan, Y. Qiu, J. Qiu and S. Yang, *ACS Appl. Mater. Interfaces,* 2013, **5**, 11249-11257.
19 D. He, X. Sheng, J. Yang, L. Chen, K. Zhu and X. Feng, *J. Am. Chem. Soc.*, 2014, **136**, 16772-16775.
20 T. S. Kang, A. P. Smith, B. E. Taylor and M. F. Durstock, *Nano Lett.*, 2009, **9**, 601-606.
21 P. Roy, S. Berger and P. Schmuki, *Angew. Chem. Int. Ed.*, 2011, **50**, 2904-2939.
22 M. S. Sander, M. J. Côté, W. Gu, B. M. Kile and C. P. Tripp, *Adv. Mater.*, 2004, **16**, 2052-2057.
23 O. K. Varghese, M. Paulose and C. A. Grimes, *Nat. Nanotech.*, 2009, **4**, 592-597.
24 L. Liu, J. Qian, B. Li, Y. Cui, X. Zhou, X. Guo and W. Ding, *Chem. Commun. (Camb.)*, 2010, **46**, 2402-2404.
25 W. Guo, C. Xu, X. Wang, S. Wang, C. Pan, C. Lin and Z. L. Wang, *J. Am. Chem. Soc.*, 2012, **134**, 4437-4441.
26 H. Huang, L. Pan, C. K. Lim, H. Gong, J. Guo, M. S. Tse and O. K. Tan, *Small*, 2013, **9**, 3153-3160.
27 G. M. Eisenberg, *Ind. Eng. Chem. Anal.*, 1943, **15**, 327-328.
28 X. Jin, X. Wang, Y. Wang and H. Ren, *Ind. Eng. Chem. Res.*, 2013, **52**, 9726-9730.
29 U. Diebold, *Surf. Sci. Rep.*, 2003, **48**, 53-229.
30 K. Pan, Q. Zhang, Q. Wang, Z. Liu, D. Wang, J. Li and Y. Bai, *Thin Solid Films*, 2007, **515**, 4085-4091.
31 V. Duzhko, V. Y. Timoshenko, F. Koch and T. Dittrich, *Phys. Rev. B*, 2001, **64**, 075204.
32 D. He, L. Wang, D. Xu, J. Zhai, D. Wang and T. Xie, *ACS Appl. Mater. Interfaces*, 2011, **3**, 3167–3171.
33 Y. Lu, Y. Lin, T. Xie, S. Shi, H. Fan and D. Wang, *Nanoscale*, 2012, **4**, 6393-6400.